



Nuclear Localization of Robo is Associated with Better Survival in Bladder Cancer

Ulrich Krafft¹ · Henning Reis² · Marc Ingenwerth² · Ilona Kovalszky³ · Markus Becker¹ · Christian Niedworok¹ · Christopher Darr¹ · Péter Nyirády⁴ · Boris Hadaschik¹ · Tibor Szarvas^{1,4}

Received: 17 April 2018 / Accepted: 9 July 2018 / Published online: 17 July 2018
© Arányi Lajos Foundation 2018

Abstract

The Slit-Robo pathway has shown to be altered in several malignant diseases. However, its role in bladder cancer is poorly understood. Therefore, we aimed to assess the tissue expression of Robo1 and Robo4 as well as their ligand Slit2 in different stages of bladder cancer to explore possible changes of Slit-Robo signalling during the progression of bladder cancer. Robo1, Robo4 and Slit2 gene expressions were analyzed in 92 frozen bladder cancer tissue samples by using reverse transcription quantitative real-time PCR. Immunohistochemical analyses were performed on 149 formalin-fixed and paraffin-embedded bladder cancer tissue samples. Results were correlated with the clinical and follow-up data by performing both univariable and multivariable analyses. Robo1 and Robo4 nuclear staining intensity was significantly higher in low stage and low grade bladder cancer. Elevated Robo1 nuclear staining was associated with better disease-specific survival (DSS) ($p = 0.045$). Similarly, stronger Robo4 nuclear staining tended to be associated with longer DSS ($p = 0.061$). We found higher Robo1 and Slit2 gene expression levels in advanced stages of bladder cancer ($p = 0.007$ and $p < 0.001$). High Slit2 gene expression was correlated with significantly shorter DSS ($p < 0.005$), while Robo1 and Robo4 gene expressions were not associated with patients' prognosis. Our results demonstrate that the nuclear expression of Robo1 and Robo4 is associated with a favourable prognosis suggesting that its translocation into the nucleus represent a posttranslational regulation process which may exhibit an antitumor effect in bladder cancer.

Keywords Bladder Cancer · Robo1 · Robo4 · Nuclear translocation · Slit2 · Prognosis · Angiogenesis

Introduction

Bladder cancer (BC) is the most common malignancy affecting the urinary tract. More than 70% of BCs are non-muscle-invasive (NMIBC) at first presentation. These tumors are

treated curatively by transurethral resection and exhibit an excellent prognosis with 5 year-survival rates of ~95%. In contrast, muscle-invasive BCs (MIBC) are commonly associated with a poorer prognosis with a 5 year-survival ranging from 50 to 60%. MIBC patients are usually treated with radical cystectomy and are at high risk of metastatic tumor progression and cancer-related death [1]. As the prognostic value of staging and grading is limited, there is a clear need for novel prognostic biomarkers to ensure adequate risk stratification for BC patients.

The secreted Slit glycoproteins and their Roundabout (Robo) transmembrane receptors playing a major role in axon guidance. Four different Robos (Robo1–4) have been described in human [2]. Robo1 and Robo4 are both receptors for Slit2. The Slit/Robo pathway is known to regulate many aspects of tissue morphogenesis and cell function such as cell migration, proliferation, adhesion and death [3, 4]. Furthermore, the Slit/Robo interaction was shown to have an important role in both pathological and physiological angiogenesis. Particularly Robo4 seems to be a key-mediator of developmental and

Electronic supplementary material The online version of this article (<https://doi.org/10.1007/s12253-018-0447-z>) contains supplementary material, which is available to authorized users.

✉ Tibor Szarvas
sztibusz@gmail.com

¹ Department of Urology, Faculty of Medicine, University Duisburg-Essen, Hufelandstr 55, 45147 Essen, Germany

² Institute of Pathology, Faculty of Medicine, University Duisburg-Essen, Essen, Germany

³ 1st Institute of Pathology and Experimental Cancer Research, Semmelweis University, Budapest, Hungary

⁴ Department of Urology, Semmelweis University, Üllői út 78/b, Budapest 1082, Hungary

pathological angiogenesis [5, 6]. Sundaresan et al. reported, for the first time, a link between Slit-Robo messaging and cancer [7]. The Slit/Robo messaging modulates several oncogenic signaling pathways that are associated with the development and progression of various cancers. In colorectal cancer Slit/Robo signaling can induce apoptosis by Slit2-Robo4 mediated suppression of netrin-1, another axon guidance protein [8, 9]. In addition it was reported that the Slit/Robo pathway inhibits cell invasion in breast cancer while interacting with β -catenin and E-cadherin [10, 11]. In accordance, altered Slit and Robo expressions were found to be associated with clinical outcome and survival of patients with various cancers. To date, little is known about the role of Slit/Robo pathway in BC and the expression of Robos and Slits has not been evaluated in BC tissues yet. The aim of the present study was to gain insight into the role of the Slit/Robo pathway in the progression and metastasis of BC and to assess their prognostic significance. Therefore, we analyzed the protein and gene expression levels of Robo1, Robo4 and Slit2 by using reverse transcription quantitative real-time PCR (RT-PCR) and immunohistochemical (IHC) analyses in a large number of BC samples. Results were compared with the clinical and follow-up data by performing both univariable and multivariable analyses. The prognostic value of the gene expression levels of these three genes were further validated on a published (TCGA) dataset of 402 BC patients (12).

Materials and Methods

Samples

Tissue samples were obtained from 220 patients who underwent surgical treatment for BC at a single academic center between 1990 and 2004. These samples included 92 snap frozen and 149 paraffin-embedded tumor samples (overlap 21 cases). Patients' characteristics are given in Tables 1 and 2. The criteria for study enrollment were histopathological diagnosis of BC, no history of other tumor, no chemotherapy before surgery, availability of sufficient tumor tissue and available follow-up data. The study was approved by the ethical board of the hospital.

RNA Isolation and Reverse Transcription

Frozen tissue samples were homogenized in QIAzol reagent (Qiagen, Hilden, Germany) and RNA isolation was performed using the RNeasy Mini kit (Qiagen) according to the manufacturer's instructions. Total RNA was quantified using an ultraviolet spectrophotometer (ND-1000; Peqlab Biotechnology GmbH, Erlangen, Germany) and the quality and integrity of samples were assessed by agarose gel electrophoresis. RNA was reverse transcribed in a final volume of 20 μ L containing 1 μ g RNA,

reverse transcription buffer, 0.5 mmol/L dNTPs, 1.8 μ mol/L oligo(dT), 10 U RNase inhibitor, and 40 U Omniscript RTase (Qiagen). Combinational DNA (cDNA) synthesis was carried out at 37 °C for 60 min. Quantitative real-time PCR was performed using 48-well plates on a StepOne real-time PCR system (Applied Biosystems, Foster City, USA). In order to provide high reproducibility, we used the pre-developed TaqMan Gene Expression Assays (Robo1: Hs01560562_m1, Robo4: Hs00219408_m1, Slit2: Hs01061407_m1). Furthermore, to allow a reliable laboratory-to-laboratory comparison of gene expression data independently of the actually used control sample, the expressions were related to Universal Human Reference RNA (Stratagene, USA), composed of pooled RNA from 10 human cell lines. We used the TATA box-binding protein gene to normalise target gene expression. Each sample was tested in duplicate. The $2^{-\Delta\Delta C(T)}$ method was used to calculate gene expression values [12].

Validation of Prognostic Value of Gene Expression Data Using the TCGA Database

We used the updated TCGA data for bladder cancer to confirm the prognostic value of Robo1, Robo4 and Slit2 (12). This data set includes the transcriptome sequencing data of 402 bladder cancer patients with available survival data. We used the OncoLnc online tool to prepare Kaplan-Meier plots and to calculate log rank tests.

Immunohistochemical Analysis

For tissue microarray (TMA) construction, hematoxylin and eosin-stained slides were established from 149 formalin fixed and paraffin embedded (FFPE) BC-tissue blocks and a pathologist (H.R.) defined representative tumor regions. Tissue cylinders with a diameter of 2 mm were then punched from selected tumor areas of each donor tissue block and brought into a recipient paraffin block. Robo1, Robo4 and Slit2 (Abcam, Cambridge, UK) IHC staining was performed on 4 μ m thick TMA sections. Automated IHC was performed using the Dako Autostainer Plus System with the anti-mouse IgG EnVision Plus detection kit (Dako) for secondary and tertiary immunoreactions. Reaction products were developed with diaminobenzidine, according to general E310 protocols. Negative control sections, with the omission of the primary antibody, were included in each run. In the case of Robo1, Robo4 and Slit2 staining, intensity was scored as 0, 1 or 2, corresponding to negative, weak and strong intensities. In case of Robo1 and Robo4 nuclear and cytoplasmatic immunostainings were separately evaluated (Table 1).

Statistical Analysis

For paired group comparisons, the nonparametric, two-sided Wilcoxon rank-sum test (Mann-Whitney test) was applied.

Table 1 Patient characteristics and Robo1, -4 and Slit2 protein expression

	Robo1 Cytoplasmic staining intensity				Robo1 Nuclear staining intensity				Robo4 Cytoplasmic staining intensity				Robo4 Nuclear staining intensity				Slit2 Cytoplasmic staining intensity													
	n	n	0-1	%	2	%	P (χ ²)	0	%	1-2	%	P (χ ²)	n	0-1	%	2	%	P (χ ²)	n	0-1	%	2	%	P (χ ²)						
Age																														
≤70	57	57	36	63	21	37	0.185	25	44	32	56	0.013	55	39	71	16	29	0.621	18	33	37	67	0.753	87	45	52	42	48	0.836	
>70	66	66	49	74	17	26		15	23	51	77		60	45	75	15	25		18	30	42	70		62	31	50	31	50		
Sex																														
Male	95	95	66	69	29	31	0.871	32	34	63	66	0.612	89	66	74	23	26	0.618	24	27	65	73	0.063	118	61	52	57	48	0.743	
Female	28	28	19	68	9	32		8	29	0	71		26	18	69	8	31		12	46	14	54		31	15	48	16	52		
Stage																														
pTa	37	37	26	70	11	30		9	24	28	76		35	31	89	4	11		5	14	30	86		38	14	37	24	63		
pT1	34	34	21	62	13	38		8	24	26	76		31	22	71	9	29		6	19	25	81		27	13	48	14	52		
pT2	29	29	21	72	8	28		10	34	19	66		25	16	64	9	36		10	40	15	60		36	20	56	16	44		
pT3	17	17	11	65	6	35		12	71	5	29		17	11	65	6	35		11	65	6	35		30	19	63	11	37		
pT4	6	6	6	100	0	0		1	17	5	83		6	4	67	2	33		4	67	2	33		16	9	56	7	44		
Non-inv.	71	71	47	66	24	34	0.455	17	24	54	76	0.014	66	53	80	13	20	0.035	11	17	55	83	<0.001	65	27	42	38	58	0.042	
Invasive	52	52	38	73	14	27		23	45	29	55		48	31	65	17	35		25	52	23	48		82	48	59	34	41		
Grade																														
G1	21	21	13	62	8	38		4	19	17	81		20	17	85	3	15		2	10	18	90		23	10	43	13	57		
G2	59	59	40	68	19	32		17	29	42	71		55	46	84	9	16		14	25	41	75		58	30	52	28	48		
G3	43	43	32	74	11	26		19	43	24	57		40	21	53	19	48		20	50	20	50		68	36	52	32	48		
Low-grade (G 1-2)	80	80	53	66	27	34	0.350	21	26	59	74	0.043	75	63	84	12	16	<0.001	16	21	59	79	0.002	81	40	49	41	51	0.665	
High-grade (G 3)	43	43	32	74	11	26		19	44	24	54		40	21	53	19	47		20	50	20	50		68	36	53	32	47		
Lymph node																														
N0/Nx/M0/Mx	114	114	80	70	34	30	0.361	36	32	78	68	0.428	106	78	74	28	26	0.653	32	30	74	70	0.376	125	62	50	63	50	0.433	
N + / M+	9	9	5	56	4	44		4	44	5	56		9	6	67	3	33		4	44	5	56		24	14	58	10	42		
missing cases	26												34												0					

Significant results ($p < 0.05$) are presented in bold

Table 2 Patient characteristics and Robo1, Robo4 and Slit2 expression

Variables	Gene expression						
	n	Robo1 gene expression median (range)	P	Robo4 gene expression median (range)	P	Slit2 gene expression median (range)	P
Age							
≤ 70	55	1.458 (0.06–7.95)	0.383	0.027 (0.000–0.270)	0.852	0.009 (0.000–0.280)	0.761
> 70	37	1.462 (0.14–16.35)		0.026 (0.01–0.170)		0.006 (0.000–0.620)	
Sex							
Male	23	1.183 (0.22–7.95)	0.882	0.035 (0.010–0.170)	0.391	0.021 (0.000–0.620)	0.119
Female	69	1.530 (0.06–16.35)		0.024 (0.000–0.270)		0.006 (0.000–0.280)	
Stage							
pTa	29	0.779 (0.06–7.14)	0.007	0.024 (0.010–0.270)	0.095	0.002 (0.000–0.070)	<0.001
pT1	17	1.183 (0.130–9.420)		0.015 (0.010–0.110)		0.003 (0.000–0.070)	
pT2	14	1.946 (0.700–8.680)		0.030 (0.000–0.190)		0.011 (0.000–0.160)	
pT3	22	2.263 (0.290–16.350)		0.043 (0.010–0.170)		0.038 (0.000–0.620)	
pT4	10	1.353 (0.480–3.170)		0.022 (0.010–0.090)		0.043 (0.010–0.110)	
Non-inv.	46	0.896 (0.060–9.420)		0.022 (0.010–0.270)		0.0025 (0.000–0.070)	
Invasive	46	1.928 (0.290–16.350)		0.032 (0.000–0.190)		0.0285 (0.000–0.620)	
Grade							
G1	15	0.779 (0.060–2.490)	0.002	0.023 (0.010–0.110)	0.269	0.002 (0.000–0.100)	<0.001
G2	35	1.272 (0.100–9.420)		0.023 (0.010–0.270)		0.003 (0.000–0.220)	
G3	42	1.946 (0.400–16.350)		0.031 (0.000–0.190)		0.030 (0.000–0.620)	
Low-grade (G 1–2)	50	0.964 (0.060–9.420)		0.023 (0.010–0.027)		0.003 (0.000–0.220)	
High-grade (G 3)	42	1.946 (0.400–16.350)		0.031 (0.000–0.190)		0.030 (0.000–0.620)	
Metastasis							
N0/Nx/M0/Mx	79	1.462 (0.060–16.350)	0.871	0.026 (0.010–0.270)	0.946	0.006 (0.000–0.620)	0.129
N + / M+	13	1.388 (0.480–4.560)		0.032 (0.000–0.090)		0.012 (0.00–0.110)	
Smoking							
yes	27	1.958 (0.130–7.950)	0.303	0.035 (0.01–0.190)	0.856	0.005 (0.000–0.620)	0.494
no	34	1.083 (0.190–9.420)		0.034 (0.010–0.160)		0.0101 (0.000–0.200)	
unknown	31						

Significant results ($p < 0.05$) are presented in bold

Associations of Robo1, Robo4 and SLIT2 IHC staining (both cytoplasmatic and nuclear) and clinicopathological variables were evaluated using the Chi-square test. Univariable disease-specific survival (DSS) and overall survival (OS) analyses were done using Kaplan–Meier log-rank test and univariable Cox analysis. For multiple analyses, the Cox proportional hazards regression model was used. In all tests $P < 0.05$ was considered to indicate statistical significance.

Results

Clinical Background

The main characteristics of the patients are demonstrated in Tables 1 and 2. In the immunohistochemistry (IHC) cohort the median follow-up time was 34 months with a maximum of 181 months. Sixty-three of 149 patients were treated by radical cystectomy, while 86 patients received transurethral

resection of the bladder (TURB). In the gene expression cohort, with available frozen tissue samples, the median follow-up time was 35 months with a maximum of 187 months. In this cohort, 45 of the 92 patients were treated by radical surgery and 46 received TURB.

Immunohistochemical Staining

Robo1 showed both cytoplasmatic and nuclear staining. Stromal cells, such as endothelial cells, fibroblasts, lymphocytes and plasma cells showed frequent positivity for Robo1. The staining pattern of Robo4 was similar to that of Robo1. Slit2 staining was visible in tumor cells, while the surrounding stromal cells remained negative.

Our analysis revealed no significant correlations between patients' age, sex or smoking habits and Robo1, Robo4 or Slit2 immunostaining (Table 3). Robo1 and Robo4 nuclear staining intensity was significantly higher in low stage and low grade cases. In accordance, higher Robo1 nuclear staining

Table 3 Cox univariable analysis

Variables	DSS - gene expression			Variables	DSS - immunostaining			
	HR	95% CI	P		HR	95% CI	P	
Age	≤ 70	ref.		Age	≤ 70	ref.		
	> 70	1.571	0.875–2.822	0.136	> 70	1.293	0.730–2.290	0.378
Sex	Female	ref.		Sex	Female	ref.		
	Male	0.469	0.252–0.871	0.017	Male	0.857	0.446–1.648	0.644
Stage	pTa - pT1	ref.		Stage	Ta - T1	ref.		
	pT2 - pT4	5.686	2.864–11.286	<0.001	T2 - T4	5.058	2.697–9.487	<0.001
Grade	G1–2	ref.		Grade	G1–2	ref.		
	G3	5.177	2.700–9.923	<0.001	G3	3.393	1.916–6.011	<0.001
Metastasis	N0/Nx/M0/Mx	ref.		LN status	N0	ref.		
	N + / M+	4.750	2.363–9.552	<0.001	N+	6.591	3.022–14.376	<0.001
Smoking	no	ref.		Smoking	no	ref.		
	yes	0.609	0.295–1.256	0.179	yes	–	–	–
Robo1 gene exp.	low	ref.		ROBO1 - Cyt.	0	ref.		
	high	1.427	0.796–2.559	0.223	0<	0.762	0.408–1.423	0.393
Robo4 gene exp.	low	ref.		ROBO1 - Nucl.	0	ref.		
	high	1.224	0.661–2.268	0.521	0<	0.749	0.562–0.999	0.049
Slit2 gene exp.	low	ref.		ROBO4- Cyt.	0	ref.		
	high	4.218	2.257–7.885	<0.001	0<	1.872	1.004–3.490	0.072
				ROBO4- Nucl.	0	ref.		
				0<	0.551	0.295–1.030	0.062	
				Slit2 - I H C	0	ref.		
				0<	0.843	0.657–1.082	0.180	

Significant results ($p < 0.05$) are presented in bold

Abbreviations: DSS - disease-specific survival HR - hazard ratio, CI – confidence interval, Ref. – referent, Cyt. - cytoplasmic, Nucl. - nuclear

scores were associated with better DSS ($p = 0.045$) (Figs. 1 and 2 and Table 3). Similarly, stronger Robo4 nuclear expression tended to be associated with longer DSS ($p = 0.061$). In contrast, Robo4 cytoplasmic staining was significantly higher in muscle-invasive and high grade tumors ($p = 0.035$ and $p < 0.001$, respectively) and the higher cytoplasmic Robo4 staining showed a trend to be associated with shorter DSS ($p = 0.074$). No such correlations were noted regarding the cytoplasmic staining of Robo1 (Table 1). Slit2 staining was higher in low stage tumors ($p = 0.042$) but showed no association with tumor grade. Slit2 staining showed no significant correlation with DSS (Fig. 3 and Table 3).

In multivariable analysis only tumor stage (>Ta-T1) remained as a significant prognostic factor for disease-specific survival (Table 4).

Gene Expression Analysis

Patients' age, sex and smoking habits showed no impact on Robo1, Robo4 and Slit2 gene expressions (Table 3). We found increasing Robo1 and Slit2 gene expression levels during the progression of BC ($p = 0.007$ and $p < 0.001$), while Robo4 showed no correlation with tumor stage or grade (Table 2). High Slit2 gene expression was correlated with significantly shorter DSS, while Robo1 and Robo4 gene expressions were not associated with patients' prognosis (Figs. 2 and 3, Table 2). In order to validate the prognostic value of Robo1, Robo4

and Slit2, we assessed their prognostic value using the updated TCGA dataset. This dataset includes transcriptome sequencing (mRNA expression) data of 402 bladder cancer patients with available survival data [2]. The results of this analysis confirmed our data by showing no prognostic significance for Robo1 and Robo4 gene expressions ($p = 0.593$ and $p = 0.328$) but a significant shorter survival for patients with high Slit2 expression ($p = 0.009$) (Supplementary Figure 1).

In multivariable analysis only presence of metastasis (regional or distant) proved to be an independent prognostic factor for disease-specific survival (Table 4).

Discussion

Patients with BC represent a clinically heterogeneous group with different risk of progression, which cannot be predicted by the histopathological examination. Therefore, to understand this heterogeneity, better insight into the molecular mechanisms involved in BC progression is needed. In the present study we found that Robo1, Robo4 and Slit2 are differentially expressed between various stages of BC. In addition, our results suggest that changes in the subcellular localization of Robo1 and Robo4 may be involved in the progression of BC.

There are conflicting data concerning the role of Slit/Robo signaling in tumorigenesis. In most cancer types, Slit/Robo mediated messaging acts as a tumor suppressor by inhibiting cell

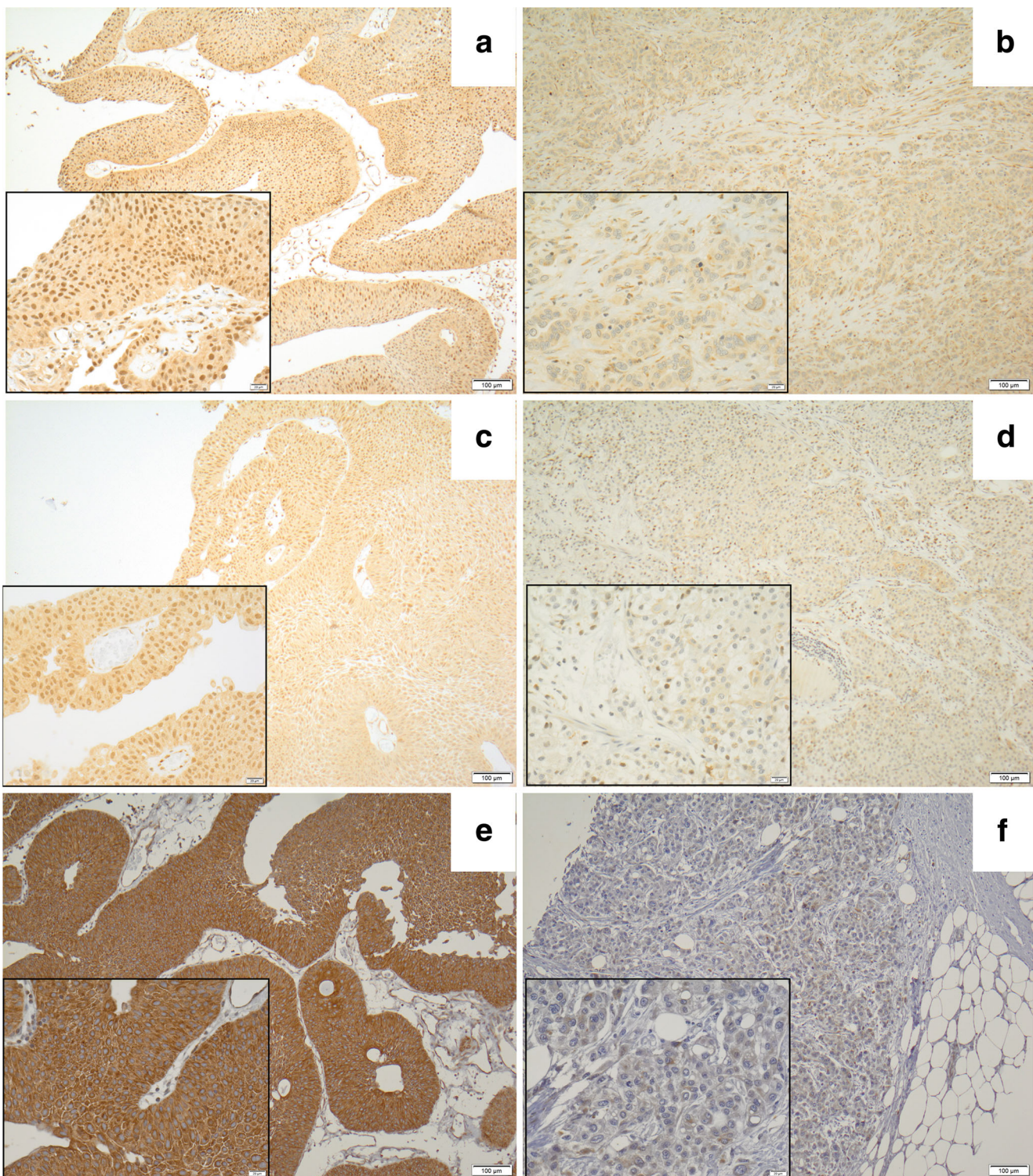
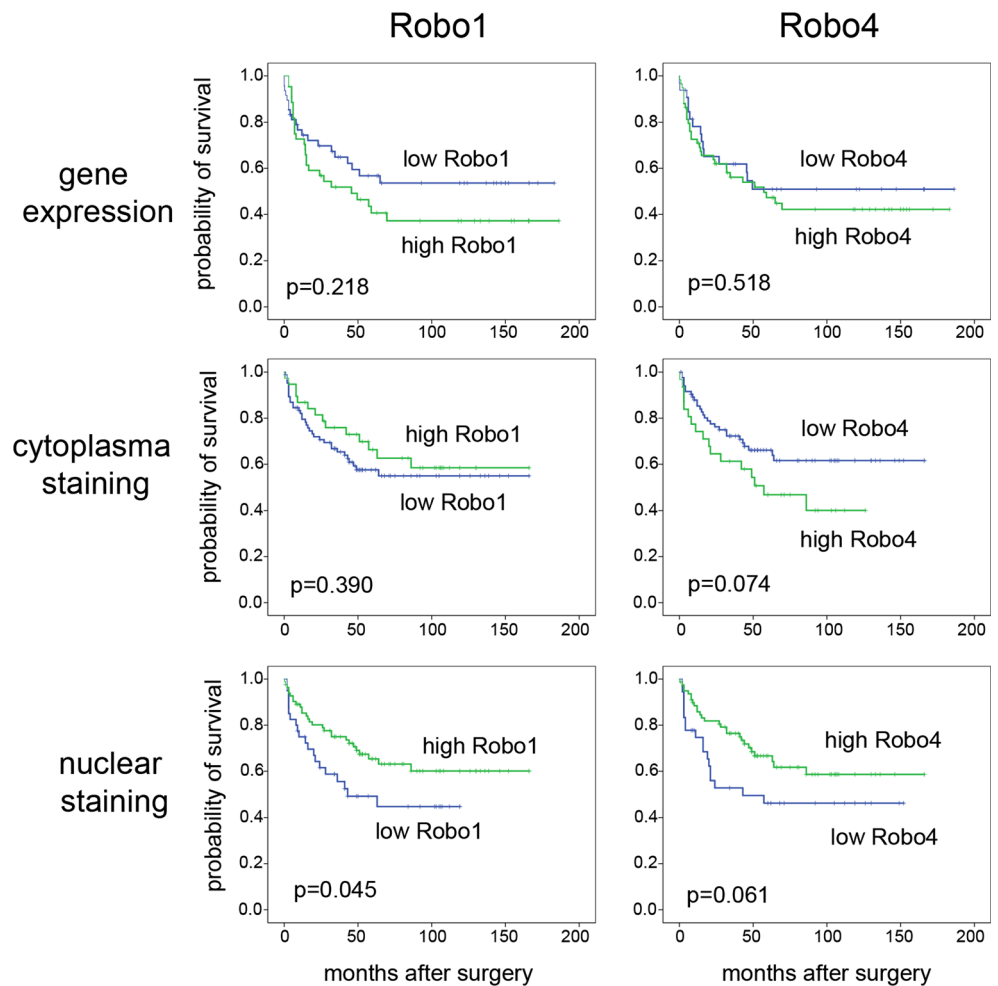


Fig. 1 Representative micrographs of Robo1 (a, b), Robo4 (c, d) and Slit2 (e, f) immunostainings. The left column (a, c, e) shows the expression in NMIBC and the right column (b, d, f) in MIBC. **a**) Shows strong nuclear Robo1-expression in NMIBC, while nuclear Robo1-reactivity is weak and focal in MIBC (**b**). The same is depicted for Robo4 in **c**) and **d**). Slit2-expression tended to be more pronounced in NMIBC (**e**) with strong cytoplasmic reactivity, while in MIBC (**f**) usually weaker immunostaining was observed. Larger photomicrographs are in 100x magnification and inset in 400x. Representative micrographs of

Robo1 (a, b), Robo4 (c, d) and Slit2 (e, f) immunostainings. The left column (a, c, e) shows the expression in NMIBC and the right column (b, d, f) in MIBC. **a**) Shows strong nuclear Robo1-expression in NMIBC, while nuclear Robo1-reactivity is weak and focal in MIBC (**b**). The same is depicted for Robo4 in **c**) and **d**). Slit2-expression tended to be more pronounced in NMIBC (**e**) with strong cytoplasmic reactivity, while in MIBC (**f**) usually weaker immunostaining was observed. Larger photomicrographs are in 100x magnification and inset in 400x

Fig. 2 Kaplan-Meier disease-specific survival curves stratified by Robo1 and Robo4 gene and protein expressions (log rank test has been performed to calculate *p*-values)



invasion and migration [5, 13, 14], with the exception of some gastrointestinal cancers. Zhou et al. showed that the expression of Slit2 and Robo1 was significantly associated with an increased metastatic risk and poor overall survival in colorectal carcinoma patients [15]. In contrast, for hepatocellular carcinoma Stella et al. found that Slit/Robo acts as an antagonist of invasive growth by inhibiting of cell migration and increasing E-cadherin mediated adhesive intercellular strength [16]. Similarly, in breast cancer Slit/Robo exhibit antitumor activity; their higher tumor tissue expressions were correlated with improved patients

survival [17, 18]. Wang et al. showed for esophageal squamous cell cancer that downregulation of Slit2 is correlated with occurrence of metastases and poor patients' survival.

There are only limited data regarding the role of Slit/Robo signaling in BC. In the only available publication, Li et al. established an in vivo model in which cultivated BC cells were transplanted into nude mice. The transplanted tumor cells were then blocked by anti-Robo1 and -4 antibodies. They found that the anti-Robo1 group showed significantly lower tumor growth suggesting Robo1 to play a proangiogenic role in BC

Fig. 3 Kaplan-Meier disease-specific survival curves stratified by Slit2 gene and protein expressions (log rank test has been performed to calculate *p*-values)

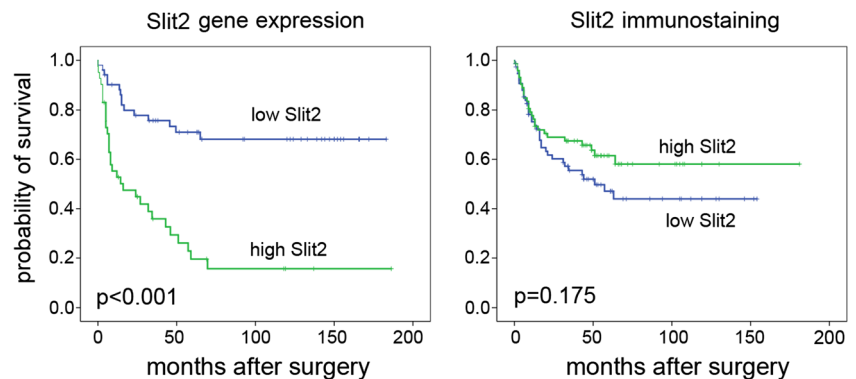


Table 4 Cox multivariable analysis

Variables		DSS - gene expression			Variables		DSS - immunostaining		
		HR	95% CI	P			HR	95% CI	P
Sex	Female	ref.			Sex	Female			
	Male	0.722	0.379–1.375	0.322		Male			
Stage	pTa - pT1	ref.			Stage	Ta - T1	ref.		
	pT2 - pT4	1992	0.677–5.864	0.211		T2 - T4	3600	1.497–8.658	0.004
Grade	G1–2	ref.			Grade	G1–2	ref.		
	G3	2038	0.831–4.998	0.120		G3	1437	0.613–3.366	0.404
Metastasis	N0/Nx/M0/Mx	ref.			Metastasis	N0/Nx/M0/Mx	ref.		
	N + / M+	3274	1.546–6.932	0.002		N + / M+	2139	0.838–5.459	0.112
Robo4 gene exp.	low				ROBO1 - Nucl.	0	ref.		
	high					0<	0.861	0.617–1.202	0.380
Slit2 gene exp.	low	ref.			ROBO4- Cyt.	0	ref.		
	high	1626	0.689–3.838	0.268		0<	1134	0.602–2.137	0.697
					ROBO4- Nucl.	0	ref.		
						0<	0.956	0.555–1.649	0.872

Significant results ($p < 0.05$) are presented in bold

Abbreviations: DSS - disease-specific survival HR - hazard ratio, CI – confidence interval, Ref. – referent, Cyt. - cytoplasmic, Nucl. - nuclear

[19]. The aim of the present study was to further determine the role of Robo/Slit signaling in BC progression by analyzing their tissue gene and protein expressions in a large number of clinical samples. During the evaluation of immunohistochemical data, we put focus on the subcellular localization of Robos as their nuclear translocation was formerly found to be of functional relevance [20]. In this regard, Seki et al. described a multistep proteolysis representing a novel post-translational regulation process for Robo1 which results in the translocation of Robo1 into the nucleus and changing its signaling function [21]. On the mRNA level, we found increasing Robo1 expression at higher stages of BC. In contrast, its nuclear protein expression decreased during tumor progression. In addition, higher Robo1 nuclear staining was significantly associated with favourable prognosis. These results suggest a clinically relevant post transcriptional regulation for Robo1 with an impact on its subcellular localization. In contrast to Robo1, the gene expression of Robo4 showed no significant changes during tumor progression but its nuclear staining intensity - similar to Robo1 - was significantly decreased in progressed stages of BC. These results, similar to those with Robo1, suggest that not the primary expression but its subcellular localization of Robo1 plays a role in the progression of BC. Furthermore, our results showing that the nuclear translocation of Robo1 and Robo4 is associated with a more favourable prognosis suggest that this mechanism may represent an intrinsic antitumor mechanism in BC. This prognostic effects, however, does not prove to be independent from tumor stage and grade and therefore Robo1 can hardly be used as prognostic factors in BC.

For Slit2, we found increased gene expression during tumor progression and an association between higher gene expression and a poor disease-specific survival. This prognostic effect could be validated by the in silico analysis of 402 BC patients (12). This prognostic effect however could not be confirmed on the protein level.

Taking together, analyzing the tissue gene and protein expression levels of Robo1, Robo4 and Slit2 for the first time, we demonstrate that nuclear expression of Robo1 and Robo4 is associated with a favourable prognosis suggesting that its translocation into the nucleus represent may exhibit an antitumor effect in BC. Overall, our protein expression data suggest a tumor suppressor role for the Robo/Slit pathway in BC. The lack of correlation between the gene expression and protein level of Robo1, Robo4 and Slit2 suggests that these molecules underlay a significant post-transcriptional regulation, which in case of Robo1 and Robo4 influences their subcellular localization. Further analyses are needed to understand the role of this mechanism in BC and to investigate the therapeutic potential of Slit/Robo pathway.

Funding This work was supported by the National Research, Development and Innovation Office – NKFIH / PD 115616. Tibor Szarvas was supported by János Bolyai Research Scholarship of the Hungarian Academy of Sciences.

Compliance with Ethical Standards

Conflict of Interest The authors declare that they have no conflict of interest.

Ethical Approval All procedures performed in studies involving human participants were in accordance with the ethical standards of the institutional and/or national research committee and with the 1964 Helsinki declaration and its later amendments or comparable ethical standards.

Informed Consent Informed consent was obtained from all individual participants included in the study.

References

- Stein JP, Skinner DG (2006) Radical cystectomy for invasive bladder cancer: long-term results of a standard procedure. *World J Urol* 24(3):296–304. <https://doi.org/10.1007/s00345-006-0061-7>
- Robertson AG, Kim J, Al-Ahmadie H, Bellmunt J, Guo G, Cherniack AD, Hinoue T, Laird PW, Hoadley KA, Akbani R, Castro MAA, Gibb EA, Kanchi RS, Gordenin DA, Shukla SA, Sanchez-Vega F, Hansel DE, Czerniak BA, Reuter VE, Su X, de Sa Carvalho B, Chagas VS, Mungall KL, Sadeghi S, Pedamallu CS, Lu Y, Klimczak LJ, Zhang J, Choo C, Ojesina AI, Bullman S, Leraas KM, Lichtenberg TM, Wu CJ, Schultz N, Getz G, Meyerson M, Mills GB, McConkey DJ, Weinstein JN, Kwiakowski DJ, Lerner SP (2017) Comprehensive molecular characterization of muscle-invasive bladder Cancer. *Cell* 171(3):540–556. <https://doi.org/10.1016/j.cell.2017.09.007>
- Wang B, Xiao Y, Ding BB, Zhang N, Yuan X, Gui L, Qian KX, Duan S, Chen Z, Rao Y, Geng JG (2003) Induction of tumor angiogenesis by Slit-Robo signaling and inhibition of cancer growth by blocking Robo activity. *Cancer Cell* 4(1):19–29
- Dickinson RE, Dallol A, Bieche I, Krex D, Morton D, Maher ER, Latif F (2004) Epigenetic inactivation of SLIT3 and SLIT1 genes in human cancers. *Br J Cancer* 91(12):2071–2078. <https://doi.org/10.1038/sj.bjc.6602222>
- Dickinson RE, Duncan WC (2010) The SLIT-ROBO pathway: a regulator of cell function with implications for the reproductive system. *Reproduction (Cambridge, England)* 139(4):697–704. <https://doi.org/10.1530/rep-10-0017>
- Kaur S, Castellone MD, Bedell VM, Konar M, Gutkind JS, Ramchandran R (2006) Robo4 signaling in endothelial cells implies attraction guidance mechanisms. *J Biol Chem* 281(16):11347–11356. <https://doi.org/10.1074/jbc.M508853200>
- Sundaresan V, Heppell-Parton A, Coleman N, Miozzo M, Sozzi G, Ball R, Cary N, Hasleton P, Fowler W, Rabbitts P (1995) Somatic genetic changes in lung cancer and precancerous lesions. *Ann Oncol* 6(Suppl 1):27–31 discussion 31–22
- Biankin AV, Waddell N, Kassahn KS, Gingras MC, Muthuswamy LB, Johns AL, Miller DK, Wilson PJ, Patch AM, Wu J, Chang DK, Cowley MJ, Gardiner BB, Song S, Harliwong I, Idrisoglu S, Nourse C, Nourbakhsh E, Manning S, Wani S, Gongora M, Pajic M, Scarlett CJ, Gill AJ, Pinho AV, Rooman I, Anderson M, Holmes O, Leonard C, Taylor D, Wood S, Xu Q, Nones K, Fink JL, Christ A, Bruxner T, Cloonan N, Kolle G, Newell F, Pinese M, Mead RS, Humphris JL, Kaplan W, Jones MD, Colvin EK, Nagrial AM, Humphrey ES, Chou A, Chin VT, Chantrill LA, Mawson A, Samra JS, Kench JG, Lovell JA, Daly RJ, Merrett ND, Toon C, Epari K, Nguyen NQ, Barbour A, Zeps N, Kakkar N, Zhao F, Wu YQ, Wang M, Muzny DM, Fisher WE, Brunnicardi FC, Hodges SE, Reid JG, Drummond J, Chang K, Han Y, Lewis LR, Dinh H, Buhay CJ, Beck T, Timms L, Sam M, Begley K, Brown A, Pai D, Panchal A, Buchner N, De Borja R, Denroche RE, Yung CK, Serra S, Onetto N, Mukhopadhyay D, Tsao MS, Shaw PA, Petersen GM, Gallinger S, Hruban RH, Maitra A, Iacobuzio-Donahue CA, Schulick RD, Wolfgang CL, Morgan RA, Lawlor RT, Capelli P, Corbo V, Scardoni M, Tortora G, Tempero MA, Mann KM, Jenkins NA, Perez-Mancera PA, Adams DJ, Largaespada DA, Wessels LF, Rust AG, Stein LD, Tuveson DA, Copeland NG, Musgrove EA, Scarpa A, Eshleman JR, Hudson TJ, Sutherland RL, Wheeler DA, Pearson JV, McPherson JD, Gibbs RA, Grimmond SM (2012) Pancreatic cancer genomes reveal aberrations in axon guidance pathway genes. *Nature* 491(7424):399–405. <https://doi.org/10.1038/nature11547>
- Gara RK, Kumari S, Ganju A, Yallapu MM, Jaggi M, Chauhan SC (2015) Slit/Robo pathway: a promising therapeutic target for cancer. *Drug Discov Today* 20(1):156–164. <https://doi.org/10.1016/j.drudis.2014.09.008>
- Prasad A, Fernandis AZ, Rao Y, Ganju RK (2004) Slit protein-mediated inhibition of CXCR4-induced chemotactic and chemoinvasive signaling pathways in breast cancer cells. *J Biol Chem* 279(10):9115–9124. <https://doi.org/10.1074/jbc.M308083200>
- Prasad A, Paruchuri V, Preet A, Latif F, Ganju RK (2008) Slit-2 induces a tumor-suppressive effect by regulating beta-catenin in breast cancer cells. *J Biol Chem* 283(39):26624–26633. <https://doi.org/10.1074/jbc.M800679200>
- Livak KJ, Schmittgen TD (2001) Analysis of relative gene expression data using real-time quantitative PCR and the 2^{−(Delta Delta C(T))} method. *Methods (San Diego, Calif)* 25(4):402–408. <https://doi.org/10.1006/meth.2001.1262>
- Huang T, Kang W, Cheng AS, Yu J, To KF (2015) The emerging role of Slit-Robo pathway in gastric and other gastrointestinal cancers. *BMC Cancer* 15:950. <https://doi.org/10.1186/s12885-015-1984-4>
- Legg JA, Herbert JM, Clissold P, Bicknell R (2008) Slits and roundabouts in cancer, tumour angiogenesis and endothelial cell migration. *Angiogenesis* 11(1):13–21. <https://doi.org/10.1007/s10456-008-9100-x>
- Zhou WJ, Geng ZH, Chi S, Zhang W, Niu XF, Lan SJ, Ma L, Yang X, Wang LJ, Ding YQ, Geng JG (2011) Slit-Robo signaling induces malignant transformation through Hakai-mediated E-cadherin degradation during colorectal epithelial cell carcinogenesis. *Cell Res* 21(4):609–626. <https://doi.org/10.1038/cr.2011.17>
- Stella MC, Trusolino L, Comoglio PM (2009) The Slit/Robo system suppresses hepatocyte growth factor-dependent invasion and morphogenesis. *Mol Biol Cell* 20(2):642–657. <https://doi.org/10.1091/mbc.E08-03-0321>
- Marlow R, Strickland P, Lee JS, Wu X, Pebenito M, Binnewies M, Le EK, Moran A, Macias H, Cardiff RD, Sukumar S, Hinck L (2008) SLITs suppress tumor growth in vivo by silencing Sdf1/Cxcr4 within breast epithelium. *Cancer Res* 68(19):7819–7827. <https://doi.org/10.1158/0008-5472.can-08-1357>
- Schmid BC, Rezniczek GA, Fabjani G, Yoneda T, Leodolter S, Zeillinger R (2007) The neuronal guidance cue Slit2 induces targeted migration and may play a role in brain metastasis of breast cancer cells. *Breast Cancer Res Treat* 106(3):333–342. <https://doi.org/10.1007/s10549-007-9504-0>
- Li Y, Cheng H, Xu W, Tian X, Li X, Zhu C (2015) Expression of Robo protein in bladder cancer tissues and its effect on the growth of cancer cells by blocking Robo protein. *Int J Clin Exp Pathol* 8(9):9932–9940
- Fujiwara M, Ghazizadeh M, Kawanami O (2006) Potential role of the Slit/Robo signal pathway in angiogenesis. *Vasc Med (London, England)* 11(2):115–121
- Seki M, Watanabe A, Enomoto S, Kawamura T, Ito H, Kodama T, Hamakubo T, Aburatani H (2010) Human ROBO1 is cleaved by metalloproteinases and gamma-secretase and migrates to the nucleus in cancer cells. *FEBS Lett* 584(13):2909–2915. <https://doi.org/10.1016/j.febslet.2010.05.009>